Recombinant immunotoxin for cancer treatment with low immunogenicity by identification and silencing of human T-cell epitopes

Ronit Mazor[a,b], Jaime A. Eberle[a,1], Xiaobo Hu[a,2], Aaron N. Vassall[a,3], Masanori Onda[a], Richard Beers[a], Elizabeth C. Lee[a,4], Robert J. Kreitman[a], Byungkook Lee[a], David Baker[c], Chris King[c], Raffit Hassan[a,d], Itai Benhar[b], and Ira Pastan[a,5]

[a]Laboratory of Molecular Biology, Center for Cancer Research, National Cancer Institute, National Institutes of Health, Bethesda, MD 20892; [b]Department of Molecular Microbiology and Biotechnology, The George S. Wise Faculty of Life Sciences, Tel Aviv University, Ramat Aviv 6998, Israel; [c]Institute for Protein Design, Department of Biochemistry, University of Washington, Seattle, WA 98122; and [d]Thoracic and Gastrointestinal Oncology, National Cancer Institute, National Institutes of Health, Bethesda, MD 20892

Contributed by Ira Pastan, March 20, 2014 (sent for review February 6, 2014; reviewed by Amy S. Rosenberg and Karl E. Griswold)

Nonhuman proteins have valuable therapeutic properties, but their efficacy is limited by neutralizing antibodies. Recombinant immunotoxins (RITs) are potent anticancer agents that have produced many complete remissions in leukemia, but immunogenicity limits the number of doses that can be given to patients with normal immune systems. Using human cells, we identified eight helper T-cell epitopes in PE38, a portion of the bacterial protein *Pseudomonas* exotoxin A which consists of the toxin moiety of the RIT, and used this information to make LMB-T18 in which three epitopes were deleted and five others diminished by point mutations in key residues. LMB-T18 has high cytotoxic and antitumor activity and is very resistant to thermal denaturation. The new immunotoxin has a 93% decrease in T-cell epitopes and should have improved efficacy in patients because more treatment cycles can be given. Furthermore, the deimmunized toxin can be used to make RITs targeting other antigens, and the approach we describe can be used to deimmunize other therapeutically useful nonhuman proteins.

deimmunization | protein engineering

Immunotoxins are chimeric proteins that combine the "magic bullet" specificity of an antibody with the high potency of a toxin. The high specificity of recombinant immunotoxins (RITs) leads to a dramatic decrease in side effects compared with chemotherapy. Moxetumomab Pasudotox (MP) is an RIT that consists of PE38, a fragment of *Pseudomonas* exotoxin A, fused to an anti-CD22 Fv (1). In a phase I trial for refractory hairy-cell leukemia (HCL), MP had an 86% response rate (2), with 46% complete remissions, and is now in phase III clinical trials (3).

Immunogenicity is a stumbling block in the clinical success of many therapeutic proteins (4). Formation of neutralizing antidrug antibodies (5) inactivates the therapeutic agent and can cause serious adverse effects. Although MP had low immunogenicity in the immune-suppressed patients of the HCL trial, some patients did eventually develop antibodies. Consequently, fewer doses could be given to these patients, leading to a reduced response rate. Additionally, RITs targeting solid tumors are less effective than MP because of their high immunogenicity in patients with normal immune systems (6, 7).

The role of helper T cells in mounting an immune response is well-established (8, 9). It was previously shown that elimination of murine T-cell epitopes reduced neutralizing antibody formation in mice (10), leading us to the hypothesis that reduction of human T-cell epitopes in the bacterial moiety of RITs would diminish its immunogenicity in humans, allowing more treatment cycles and better antitumor responses, as previously attempted for other therapeutic proteins like erythropoietin (11).

To circumvent the immunogenicity of PE38, we previously used peptide pools to map the approximate location of the T-cell epitopes and found an immunodominant and promiscuous epitope that stimulated T cells in 42% of all donors (12). Here, we have done high-resolution mapping of the epitopes and used this information to mutate and suppress seven additional epitopes. We used this information to construct a mutant RIT that has a 93% reduction in T-cell epitopes, high cytotoxic activity in vitro against leukemia cell lines and cells from patients, and excellent antitumor activity and low nonspecific toxicity in mice.

Results

Identification of T-Cell Epitopes in PE38. To identify the T-cell epitopes in PE38, we incubated peripheral blood mononuclear cells (PBMCs) from 50 normal donors and 16 immunotoxin-treated patients with an RIT for 14 d followed by restimulation with 111 overlapping peptides spanning the sequence of PE38. Responses were measured by an interleukin (IL)-2 enzyme-linked immunosorbent spot (ELISpot). Heat maps demonstrating responses of the T cells of 50 normal donors and 16 patients with anti-PE38 antibodies are shown in Fig. 1 *A* and *B*.

In this study, we define an epitope as a contiguous 9 amino acid region within a peptide that activates T cells in 5 donors or

Significance

Recombinant immunotoxins have produced complete remissions in leukemia patients where many doses can be given but are less active in patients with solid tumors because their immune system makes antidrug antibodies, which inactivate the immunotoxin. To suppress the immune response, we have identified and largely silenced the T-cell epitopes responsible for the immune response. A redesigned immunotoxin with T-cell epitope mutations is highly cytotoxic to cell lines and to cells isolated from cancer patients and produces complete remissions in mice with human cancer xenografts. The approach described can be applied to deimmunize other therapeutically useful foreign proteins.

Author contributions: R.M., I.B., and I.P. designed research; R.M., J.A.E., X.H., A.N.V., M.O., R.B., E.C.L., and R.J.K. performed research; R.J.K. and R.H. contributed new reagents/analytic tools; R.M., J.A.E., A.N.V., M.O., B.L., D.B., and C.K. analyzed data; R.M., I.B., and I.P. wrote the paper; B.L. analyzed protein structure and designed mutations; D.B. and C.K. analyzed protein structure and designed mutations; and I.P. conceived the project.

Reviewers: A.S.R., U.S. Department of Health and Human Services; K.E.G., Dartmouth College.

The authors declare no conflict of interest.

[1]Present address: Columbia University Medical Center, College of Physicians and Surgeons, New York, NY 10032.

[2]Present address: Department of Biotechnology, University of South China, Hangyeng 421001, People's Republic of China.

[3]Present address: Yale Medical School, New Haven, CT 06510.

[4]Present address: Georgetown University School of Medicine, Washington, DC 20057.

[5]To whom correspondence should be addressed. E-mail: pastani@mail.nih.gov.

This article contains supporting information online at www.pnas.org/lookup/suppl/doi:10.1073/pnas.1405153111/-/DCSupplemental.

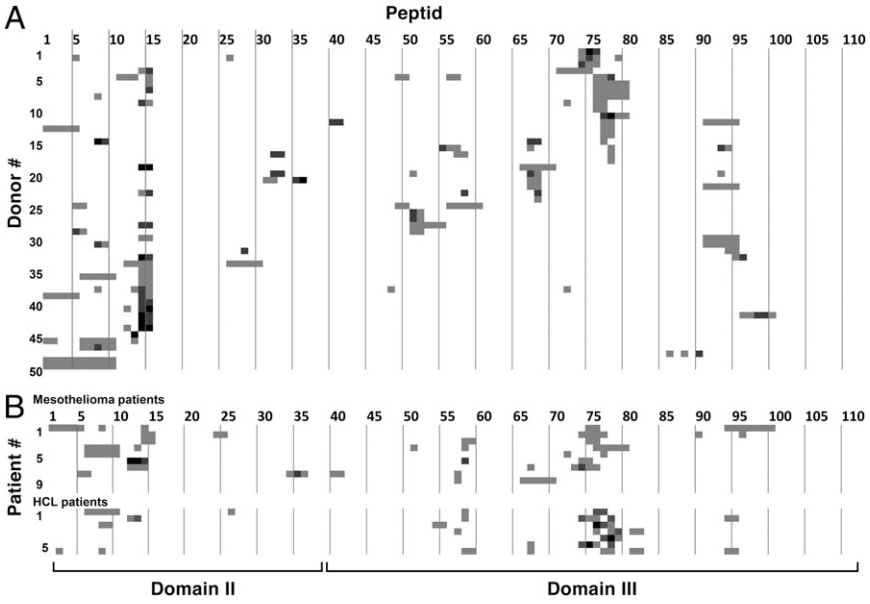

Fig. 1. T-cell epitope heat map. Visual illustration of (*A*) donor (n = 50) and (*B*) patient (n = 16) responses to PE38 peptides. Cells were stimulated and expanded with whole RIT for 14 d and restimulated with PE38 peptides. T-cell responses were measured using IL-2 ELISpot, normalized to total spots per donor and put in groups of black (>20% of spots), dark gray (10–20% of spots), gray (3–10% of spots), and white (<3% of spots and 80 SFCs per 1E6 cells). Samples were clustered using automatic sorting based on the responsiveness to the peptides. (*B*) Patient samples are separated into mesothelioma and HCL cohorts. Epitope screening was repeated once for all donors and patients.

more of our 50-donor cohort. We found eight major epitopes in PE38 that account for 93% of the responses. They are ranked by response frequency and magnitude of response in Table 1. The overlapping peptides 14 and 15 (epitope 1) had the strongest and most frequent responses. Epitope 2 spans five peptides; to simplify analysis, we divided it into two subepitopes: peptides 77–78 (2A) and peptides 75–76 (2B). Some donors responded to both 2A and 2B epitopes whereas others responded to only one. Epitope 6 (peptides 93–96) and epitope 8 (peptides 56–59) were also divided into two subepitopes.

To compare the results from naive donors to immunotoxin-treated patients, we used two patient cohorts that made neutralizing antibodies against the RIT. The patients' DRB1 HLA alleles are shown in Table S1. We found that the same epitopes identified in the donor cohort were also present in the patient cohorts. One cohort was from mesothelioma patients treated with SS1P (anti-mesothelin Fv fused to P38) (13); the other was from leukemia patients treated with MP. The naive donor epitope responses ranged from one to four epitopes per donor, with an average of 2.1; the patient responses ranged from one to seven per patient, with a higher average of 3.4 ($P < 0.001$ in Student t test). This result suggests that some responses in the naive population are too weak to be detected by our method and are amplified after exposure to immunotoxin. Importantly, the patient samples did not identify any major epitopes that were not identified using the donor cohort.

Amino Acids Required for T-Cell Activation. PE38 contains domains II and III of *Pseudomonas* exotoxin. Domain II is unnecessary for cytotoxic activity (14) and is absent in the current generation of immunotoxins. To identify amino acid variants that silence the epitopes in domain III, we synthesized a set of domain III peptides with alanine replacing key amino acids. All variants were analyzed in silico using an HLA binding algorithm [Immune Epitope Database (IEDB)] (15) for their ability to bind to 13 major HLA groups. Variants predicted to have increased binding to at least six HLA alleles were omitted from the screen. We evaluated the mutant peptides for T-cell activation by IL-2 ELISpot using all PBMCs that responded to the parent peptides. The number of spots for each variant peptide was normalized to the parent peptide so that wild-type (WT) peptides were 100% for each donor. Fig. 2 *A*–*F* shows cumulative responses of several donors to the mutant peptides. The different shades of gray in each bar represent responses of different donors, and the height of the bar represents the sum of the responses. Epitopes 2A and 2B were scanned separately to cover the 9-mer core of all five

Table 1. Epitopes summary

Epitope ranking	Peptide no.	Sequence	Responses: Donors (n = 50)	Responses: Mesothelioma (n = 9)	Responses: HCL (n = 7)	Inactivating mutations	Relative cytotoxic activity*, %
1	13–15	LVALYLAARLSWNQV	21	6	1	Domain II deletion	100
2A	77–78	GALLRVYVPRSSLPG	14†	3†	6†	R505A	100
2B	74–76	IRNGALLRVYVPRSS	10†	6†	5†	R494A	21–36
3	8–9	RQPRGWEQLEQCGYP	9	3	3	Domain II deletion	100
4	5–6	LPLETFTRHRQPRGW	10	2	0	Domain II deletion	100
5	67–68	WRGFYIAGDPALAYG	8	2	2	L477H	100
6 A+B	93–96	GPEEEGGRLETILGWPLA	8	1	2	L552E	100
7	51–52	TVERLLQAHRQLEER	5	1	0	R427A	100
8 A+B	56–59	FVGYHGTFLEAAQSIVFG	5	5	4	F443A	>100

Sites of mutagenesis are underlined.
*Activity for a single point mutation in CD22 targeting RIT was evaluated in the CA46 cell line.
†Donors and patients that responded to epitope 2A overlap with the patients and donors that responded to 2B.

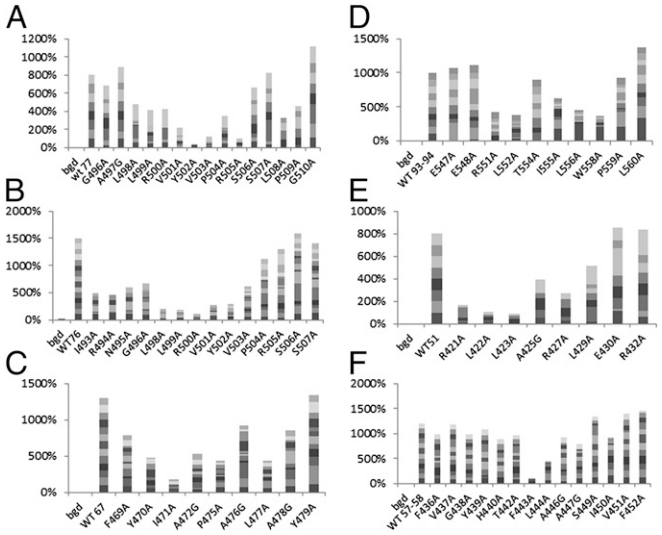

Fig. 2. Alanine scanning mutagenesis for epitopes 2A, 2B, 5, 6, 7, and 8. T-cell cumulative response for alanine variant peptides was evaluated using IL-2 ELISpot, and the SFC responses of each donor were normalized to the response of parent peptide (WT). Different shades of gray in each bar represent responses of different donors, and the height of the bar represents the sum of the responses. Small bars indicate mutants that diminish the epitope. (*A*) Epitope 2A comparing alanine peptide variants with peptide 77 (n = 8). (*B*) Epitope 2B comparing alanine peptides with peptide 76 (n = 15). (*C*) Epitope 5 comparing alanine peptide variants with peptide 67 (n = 13). (*D*) Epitope 6 comparing alanine peptide variants with 18-mer peptide 93–94 (n = 10). (*E*) Epitope 7 comparing alanine peptide variants with peptide 51(n = 8). (*F*) Epitope 8 comparing alanine peptide variants with 18-mer peptide 57–58 (n = 12). Alanine scans for all epitopes were run in quadruplicates and repeated once.

peptides that gave responses. Y502A diminished the responses of both epitopes (Fig. 2 *A* and *B*). For epitopes 5 and 7, alanine mutants were compared with peptides 67 and 51, respectively, and I471A and L423A had the lowest T-cell response (Fig. 2 *C* and *E*). To cover all 9-mer cores in epitopes 6 and 8 that contained four positive peptides, we synthesized 18-mer WT and alanine variants. We found that L552A was the most effective in lowering the response in epitope 6 (Fig. 2*D*) and that F443A was best for epitope 8 (Fig. 2*F*).

Construction of a Deimmunized RIT. Based on the alanine scan results, mutant RITs were constructed, and their activity was examined. Each alanine mutation was cloned into the HA22-LR plasmid. The cytotoxic activity of each mutant was compared with the parent HA22-LR. If the mutant protein aggregated or had low cytotoxic activity, other amino acid substitutions were evaluated. The alternative amino acids were chosen by examining the protein crystal structure (PBD ID code 1IKQ) (16) and using T-cell–binding predictions. For epitope 6, we used the recently developed ROSETA protocol, an energy algorithm structure-based deimmunization protocol to identify the L552E mutation (17). All active mutants were evaluated for their ability to diminish T-cell responses.

We constructed 40 mutant RITs. Yields of purified protein, calculated accessible surface areas (18, 19) of WT amino acid residues, and cytotoxic activity of each RIT are shown in Table S2. Active RITs were evaluated by IL-2 ELISpot following PBMC stimulation with the mutant RIT to ensure that the variant had decreased T-cell activation.

Construction and Characterization of LMB-T18. To construct a mutant with high cytotoxic activity and low immunogenicity, we used a stepwise approach, adding one mutation at a time. The best mutant, deimmunized RIT (LMB-T18), contains six point mutations: R505A, R494A, L477H, L552E, R427A, and F443A, corresponding to epitopes 2A, 2B, 5, 6, 7, and 8, respectively (Fig. 3*B*). To improve cytotoxic activity, we inserted a Gly-Gly-Ser peptide linker after the furin cleavage site because we found that this insertion improved cytotoxic activity of RITs targeting mesothelin (20). Fig. 3*C* shows the size and purity of LMB-T18 on SDS/PAGE.

Cytotoxic Activity of LMB-T18. Cytotoxicity assays of LMB-T18 were performed on four CD22-expressing cell lines and compared with the cytotoxic activity of MP (Fig. 4 *A* and *B*). LMB-T18 is very potent, with an EC_{50} < 10 pM in all cell lines. Compared with MP, LMB-T18 has a small increase of 53% in activity in CA46 cells, 54% in Daudi cells, and >200% in HAL-01 cells (P = 0.2, 0.06 and 0.01, respectively, in Student t test); however, in Raji cells, LMB-T18 has a 52% activity decrease (P = 0.3 in Student t test). The decrease in activity in Raji cells is probably due to the domain II deletion (14). The stability of LMB-T18 was compared with MP by heating samples for 15 min at various temperatures and, after cooling, measuring residual cytotoxic activities (Fig. 4*C*) on Raji cells. MP lost 50% of its activity after a 15-min incubation at 56 °C. Unexpectedly, LMB-T18 is more heat-resistant (P < 0.05 in Student t test); it lost only 50% of its activity after a 15-min incubation at 70 °C. To determine activity on patient cells, we used cells from seven HCL and six chronic lymphocytic leukemia (CLL) patients. Fig. 4 *D* and *E* shows that LMB-T18 is more active than MP on CLL cells, though not significantly different on HCL cells.

Antitumor Activity in Mice. Severe combined immunodeficient (SCID) mice were implanted with CA46 cells; 7 d later, when tumors reached over 100 mm^3 in size, the mice were treated intravenously. Mice receiving 5.0 mg/kg were treated four times, on days 7, 9, 11, and 16, and the higher dose group was treated with 7.5 mg/kg three times on days 7, 9, and 11. Marked tumor regressions were observed in all mice (Fig. 5*F*), with only minor weight loss (average of 6%). Five of seven mice treated with 5.0 mg/kg maintained complete tumor regression on day 33, and three of seven mice maintained complete tumor regression in the 7.5 mg/kg group. To assess the nonspecific toxicity of LMB-T18, six tumor-bearing mice were treated i.v. with two doses of 10 mg/kg every other day; one mouse showed severe weight loss and was euthanized.

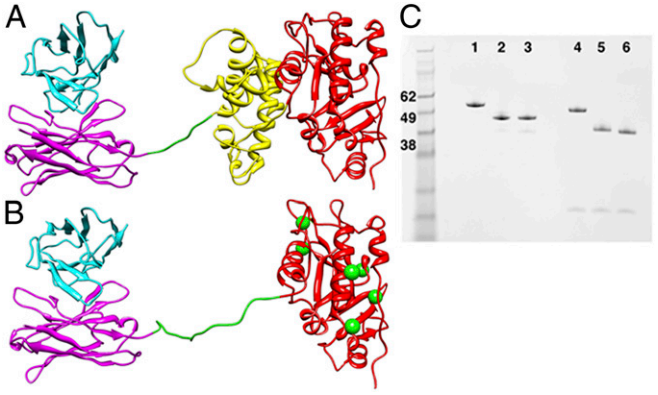

Fig. 3. Structural models of RIT and LMB-T18 and SDS/PAGE. V_L (cyan) and V_H (magenta). Domain II of the toxin (yellow) and domain III (red). T-cell point mutations (highlighted in green, from top left to bottom right: R494A, F443A, R427A, L477H, L552E, and R505A). (*A*) Moxetumomab Pasudotox. (*B*) LMB-T18. (*C*) SDS/PAGE showing purified RITs. MP, HA22-LR, and LMB-T18 in nonreducing conditions (lanes 1–3); MP, HA22-LR, and LMB-T18 in reducing conditions (lanes 4–6).

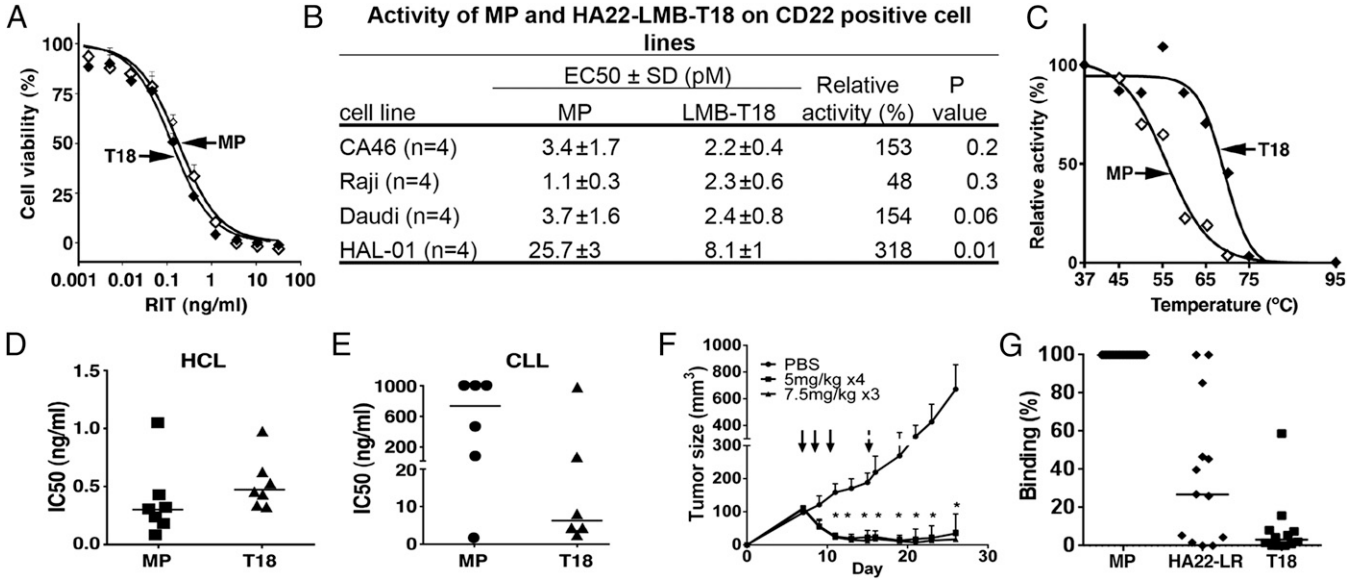

Fig. 4. Characterization and properties of LMB-T18 in vitro. (*A*) Representative cytotoxic activity in CA46 cells using WST-8 cell viability assay. (*B*) Summary of cytotoxic activity on various $CD22^+$ cells using WST-8 cell viability assay and statistical significance in two-tailed Student *t* test. (*C*) Cell viability of Raji cells after treatment with LMB-T18 that was heated to various temperatures. Relative activity was calculated based on IC_{50} of each RIT in each temperature, normalized to the activity of the RIT at 37 °C. (*D* and *E*) Activity of MP and LMB-T18 in patient cells. Cells from seven HCL and seven CLL patients were treated with MP or LMB-T18. The IC_{50} of the RIT in HCL patients (*D*) and of CLL patients (*E*) was evaluated using ATP cell viability assay. Center values are medians. (*F*) Effect of LMB-T18 on tumor size in xenograft mouse model after four injections of 5 mg/kg and three injections of 7.5 mg/kg, respectively or PBS-0.2% human serum albumin. Arrows represent days of injection for all dose groups. Broken arrow for additional injection of 5 mg/mL group. $*P > 0.01$ in one-way ANOVA. Error bars indicate SD. (*G*) Human antigenicity of LMB-T18. Binding of MP, HA22-LR, or LMB-T18 to antibodies in human sera was analyzed in a displacement assay. IC_{50} values from the binding curves were calculated, and binding ratio was calculated from each IC_{50} of each serum sample. Center values are medians. $P < 0.05$ in one-way ANOVA test. All three groups were significantly different.

LMB-T18 Has Greatly Diminished T-Cell Activation. To determine whether LMB-T18 had a decrease in T-cell stimulation or whether new T-cell epitopes were created by the mutations, we stimulated PBMCs from the highest responder donors ($n = 13$) and HCL and mesothelioma patients ($n = 7$) with MP or LMB-T18. Cells were restimulated with the 39 newly designed peptides representing the differences between MP and LMB- T18. Fig. 5 shows a decrease of 90% in donor T-cell activation ($P < 0.0001$ in Student *t* test). Even in patients with activated T cells, there was an 83% decrease ($P < 0.0001$ in Student *t* test). Furthermore, we found that no new epitopes were created by the mutations.

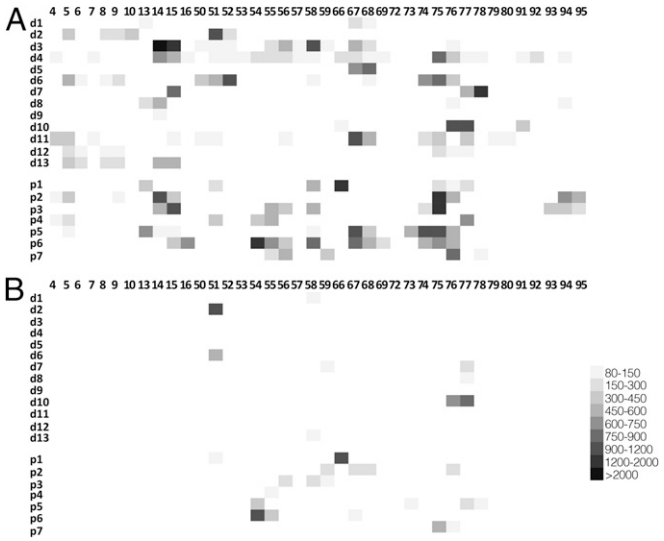

Fig. 5. Visual illustration of T-cell response to MP and LMB-T18 in 20 donors and patients. Cells from 13 naive donors (d1–d13) and 7 previously treated patients (p1–p7) were stimulated with either MP or LMB-T18 and expanded for 14 d. Cells were restimulated with either 39 WT peptides or 39 newly designed peptides representing the differences between MP and LMB-T18, respectively. (*A*) T-cell activation with MP stimulation and WT peptides. (*B*) LMB-T18 stimulation and mutant peptides. Color code scale of SFC per 1×10^6 cells is shown on the right.

LMB-T18 Has Reduced Binding to Antisera from Patients. The antigenicity of LMB-T18 was evaluated by comparing the reactivity of MP, HA22-LR, and LMB-T18 with serum from patients with neutralizing antibodies to MP. Binding was measured using immunocytochemistry (ICC)-ELISA with serum from 13 MP-treated patients and is shown in Fig. 4*G*. We found that, like HA22-LR, LMB-T18 had a significantly reduced binding to serum compared with MP ($P < 0.001$, one-way ANOVA). This result was expected because the deletion of domain II eliminated several B-cell epitopes in MP. We also found that LMB-T18 had significantly lower binding compared with HA22-LR ($P < 0.001$, one-way ANOVA), indicating that the mutations in LMB-T18 reduced the binding to antisera.

Discussion

We have identified and largely silenced all major T-cell epitopes in a highly active immunotoxin and shown that this new RIT has high cytotoxic and antitumor activity. We previously showed that domain II of PE could be deleted without loss of cytotoxic activity. By deleting domain II and inserting six mutations in domain III, we have achieved a 93% decrease in T-cell epitopes.

To identify the T-cell epitopes, we assessed T-cell responses using an ELISpot assay, which measured IL-2 production (12, 21). We observed a significant T-cell response in all 50 PBMC samples, demonstrating the robustness of the assay. To assess T-cell stimulation, we initially measured IL-2, IL-4, and IFN-γ

and found that all three gave responses but that IL-2 had the strongest response and the lowest background. It was shown previously in vaccination studies that IL-2 is a reliable indicator of CD4 T-cell activation whereas IFN-γ is more variable (22).

Epitope mapping using naive samples identifies antigen-specific naive T cells whereas epitope mapping of patients with antibodies identifies memory T cells (23). We obtained samples from nine mesothelioma patients, previously treated with SS1P, who had high levels of antidrug antibodies. We mapped their epitopes and observed more epitopes per patient than in the naive donors, but no new epitopes were found. It seems likely that the T cells from patients with antibodies are memory T cells, that they are much more abundant in the peripheral blood than naive cells, and that the epitopes they bind to are the same epitopes that initiated the memory responses. We should be able to confirm this hypothesis by characterizing the activated cells with memory and naive cellular markers staining in flow cytometry.

Remarkably, despite the fact that most of the patients had more responses than the naive donors, no new epitopes were identified by screening patient PBMCs. This result confirms that the epitope map created from screening of 50 naive donors provides comprehensive coverage of the T-cell epitopes and establishes that mutating these epitopes will be effective for patients from diverse HLA haplotypes.

Previously, we identified an immunodominant epitope in PE38 (12). Here, we identify the other seven epitopes in the toxin. Another study, which used a ^{3}H-Thymidine incorporation assay without T-cell expansion, identified only three T-cell epitopes (24); two of these epitopes are the same as our epitopes 1 and 2. The third in peptide 65 was not found in either normal or patient cohorts in our study. We hypothesize that peptide 65 is not generated by processing of the immunotoxin and is not a functional epitope and that the in vitro expansion step in our protocol eradicated this false positive.

PE38 comprises domains II and III (25) (Fig. 3*A*). Weldon et al. reported that most of the amino acids in domain II could be deleted without major loss of cytotoxic activity (14). This deletion eliminates immunodominant epitope 1 and epitopes 3 and 4 (Fig. 3*B*). The heat map in Fig. 1 shows that elimination of domain II eliminates 48% (122/256) of all responses, including 85% (11/13) of the strong responses. Here, we identified five major epitopes in domain III, which account for an additional 45% of the responses. For each epitope, we performed an alanine scan to identify amino acids that, when mutated, diminished the epitope. Three of the epitopes were complex (epitopes 2, 6, and 8) because T-cell stimulation was produced by more than two overlapping peptides. To simplify analysis of these complex epitopes, they were divided into two subepitopes (2A, 2B, etc.). For epitopes 2A and 2B, we were unable to find a mutation that eliminated both epitopes and still produced an active immunotoxin. Therefore, we used two mutations, R505A and R494A, to diminish this epitope.

To make LMB-T18 RIT, we used the HA22-LR scaffold with the addition of a GGS peptide linker. We introduced six point mutations—R505A, R494A, L477H, R427A, L552E, and F443A—to make LMB- T18. LMB-T18 had excellent cytotoxic activity in several CD22-positive cell lines, with IC_{50}s less than 10 pM, and produced complete remissions in mice with lymphoma xenografts. Because our ultimate goal is to use LMB-T18 to treat hematological malignancies in humans and because cell lines do not always reliably predict activity in patients, we evaluated the cytotoxic activity of LMB-T18 in cells from seven HCL and six CLL patients and found that it was extremely active.

One major concern of removing T-cell epitopes by point mutations is the formation of new epitopes or the emergence of cryptic epitopes that were suppressed by stronger epitopes (26). We examined the RITs with single and multiple mutations and did not find new epitopes, probably because alanine substitutions are likely to deactivate epitopes by disrupting peptide-HLA binding or by disrupting binding to the T-cell receptor. Our result is in agreement with the findings of Yeung et al., who found that elimination of murine T-cell epitopes in human IFN-β did not result in a response directed at the subdominant epitope (10). It is theoretically possible that point mutations could lead to alternative processing and formation of new epitopes. It appears that this risk did not happen because stimulation of several donors with an RIT containing point mutations and restimulation with all 22 peptide pools did not show a different epitope pattern than stimulation with WT.

Interestingly, stimulation of samples using LMB-T18 showed a significantly decreased T-cell response in all of the epitopes compared with the parent peptides. Accounting for response strength and frequency, LMB-T18 had a decrease of 90% in T-cell activation compared with MP in naive donors. We found that mutant peptides were completely nonstimulatory in some donor and patient samples whereas other samples only showed a reduction in T-cell activation as a response to the deimmunization. This finding is probably due to the HLA variability among the samples. We do not suspect that the weak responses to peptides in LMB-T18 are a result of an enhanced cytotoxic activity of LMB-T18 that kills $CD22^{+}$ presenting cells. In this assay, PBMCs were stimulated with extremely high RIT concentrations (>5,000-fold the IC_{50} of either RIT), which should kill all $CD22^{+}$ cells in the mixture. This fact indicates that the processing and presenting that occur in our assay are not by B cells. To completely eliminate epitopes for the entire cohort, additional mutations may be required. Liu et al. (27) previously identified and silenced several human B-cell epitopes in PE38 by alanine mutations. Unexpectedly, we found that two of the mutations that diminished T-cell epitopes, R505A and R427A, also diminished B-cell epitopes (27). Because arginine residues are often highly exposed and commonly part of a B-cell epitope, it was not surprising that mutating R to A diminished the B-cell epitopes. Out of the six T-cell mutations that we identified, R505 and R427 have a very high accessible surface areas (150 Å and 142 Å, respectively) and are located on the surface of the protein (18, 19). The fact that LMB-T18 contains two mutations that also diminish B-cell epitopes explains the reduction in binding to patients' serum observed in the antigenicity assay compared with HA22-LR.

The next step will be to make RITs in which the mutations silencing T- and B-cell epitopes are combined in one molecule, assuming that no single approach will be sufficient to suppress all immune responses. Before developing such a molecule, one would need to be sure that the B-cell epitope mutations do not create new T-cell epitopes, and vice versa.

In conclusion, we have identified the major T-cell epitopes in PE38, including an immunodominant promiscuous epitope, and diminished or, in some cases, completely eliminated the epitopes while maintaining good cytotoxic activity, stability, and antitumor activity. Immunotoxins with these mutations should be more effective in cancer treatment because more treatment cycles can be given.

Materials and Methods

Human Donor PBMC Samples. Apheresis samples from patients treated with a PE38-containing RIT or normal donors were collected under research protocols approved by the National Institutes of Health (NIH) Review Board (08-C-0026 and 99-CC-0168, respectively), with informed consent. PBMCs were isolated using gradient-density separation by Ficoll-Hypaque (GE Healthcare) and frozen in 10% human AB serum (Gemini) RPMI media (Lonza) with 7.5% (3.75 mL/50 mL) DMSO (Cellgro). They were stored in liquid nitrogen. HLA typing was performed with PCR sequence-specific primers by the HLA typing unit at NIH.

Peptide Synthesis. Peptides for T-cell epitope mapping were previously described (12). Peptides with mutations were made by American Peptides and purified to 95% homogeneity.

In Vitro Expansion of PE38-Specific Cells and ELISpot Assay. In vitro expansion using whole RIT and T-cell activation detection using IL-2 ELISpot were

performed as previously described (12). Each assay was performed in quadruplicate. For T-cell epitope mapping, positive pools were fine screened to identify the individual immunogenic peptides. The threshold for a positive response included three factors. A response was considered positive if (*i*) the value was ≥80 spot-forming cells (SFCs) per 10^6 cells, (*ii*) the value was more than three times that of the negative control, and (*iii*) the spots in the pool made up more than 3% of all of the spots for that donor. This threshold provided reproducible responses for all donors.

Prediction of Point-Mutation Candidates. To narrow down the number of peptide variants, we used the prediction software Immune Epitope Database (IEDB; http://tools.immuneepitope.org) (28). We used the MHC II prediction tool and submitted the amino acid sequence of the epitope containing peptides 13 times, once for each major HLA group (DRB_101, _301, _401, _701, _801, _901, _1001, _1101, _1201, _1301, _1401, _1501, and _1601). High-affinity binding candidates were predicted and omitted from the alanine scan if they had an increased predicted binding of twofold (or more) in at least six HLA groups.

Construction, Expression, and Purification of RIT. MP, HA22-LR, and mutant RITs with single-point mutations thereof are composed of a heavy-chain Fv fused to LR-PE24 (VH-PE24) disulfide-linked to the light-chain Fv (VL) (14). The different mutations were introduced into the parent expression plasmid (MP VH-PE24) using PCR overlap extension. The resulting PCR products were cloned back into the parent plasmid, and the mutations were confirmed by DNA sequencing. RITs that contained more than one mutation and a GGS linker were synthesized by GeneScript and cloned into the expression plasmid (MP VH-PE24). All RITs were purified by a standard protocol (29).

Antigenicity Assay. Binding of MP, HA22-LR, and LMB-T18 to antibodies present in sera from patients was measured as previously described (30). Briefly, mesothelin-rFc was added to an ELISA plate (100 ng in 50 μL PBS per well) and incubated overnight at 4 °C. After washing, an anti-mesothelin RIT, SS1P (which contains PE38, 100 ng in 50 μL PBS per well) was added for 1 h. In separate tubes, appropriate diluted sera were mixed with 2 ng/mL MP, HA22-LR, or LMB-T18 and incubated overnight at 4 °C. After washing the plate, 50 μL of immunotoxin–antibody mixtures were transferred to each well. The human antibodies not bound to MP, HA22-LR, or LMB-T18 were captured by SS1P and detected by HRP-conjugated rabbit anti-human IgG Fc, followed by TMB substrate kit (Pierce). From the binding curves, IC_{50} values were calculated. The IC_{50} values indicate the concentration of RIT (MP, HA22-LR, or LMB-T18) that inhibits 50% of the antibody reactivity with SS1P. The binding ratio was calculated from each IC_{50} value. Human sera were obtained under a National Institutes of Health Institutional Review Board-approved protocol (08-C-0026).

Activity Assays. ***WST8 assay.*** Cell viability was evaluated on $CD22^+$ human Burkitt's lymphoma cell lines (CA46, Raji, and Daudi) and an acute lymphoblastic leukemia cell line (HAL-01) using a WST8 cell-counting kit (Dojindo Molecular Technologies) according to manufacturer instructions and as previously described (12). Cell lines were obtained from ATCC and tested negative for mycoplasma contamination.

ATP assay. Viability of leukemia cells was measured by the ATP levels using the CellTiter-Glo Luminescent Cell Viability Assay (Promega) according to manufacturer protocol.

Thermal-Stability Assessment. RITs were heated for 15 min at various temperatures as previously described (12). Viability was determined by WST8 assay. IC_{50} was calculated for each temperature using a four-parameter linear curve fit, and relative activity to 37 °C IC_{50} was calculated.

Mouse Xenograft Antitumor Activity and Dosing. Female SCID mice (6 wk old, 18–22 g) were injected s.c. in the flank with 1×10^7 CA46 cells. After 7 d, when the tumors reached 100 mm^3, three groups of mice with similar average weight and tumor size were injected i.v. with 5 mg/kg LMB-T18 in PBS containing 0.2% human serum albumin on days 7, 9, 11, and 16 or 7.5 mg/kg on days 7, 9, and 11 or 10 mg/kg on days 7 and 9. Body weight and tumor size were observed for 30 d. Mice were euthanized if they experienced rapid weight loss or tumor burden greater than 10% body weight. Animal experiments were performed under National Cancer Institute Animal Care and Use Committee-approved protocols. No animals were excluded from statistical analysis. Tumor-size evaluation was evaluated blindly.

Statistical Analysis. A nonparametric Friedman's test was used to compare the screen results of the 111 peptides for 50 donors. $P < 0.05$ was considered statistically significant. Two-tailed Student *t* test and one-way ANOVA were used for all other analyses.

ACKNOWLEDGMENTS. We thank Laiman Zhang and Emily Mason-Osann for help with animal experiments. We also thank Dr. Jay Berzofsky, Dr. Yoram Reiter, Dr. John E. Weldon, and Dawn Walker for reviewing the paper and providing helpful advice. This research was supported by the Intramural Research Program of the National Institutes of Health, National Cancer Institute, Center for Cancer Research.

1. Kreitman RJ, Pastan I (2011) Antibody fusion proteins: Anti-CD22 recombinant immunotoxin moxetumomab pasudotox. *Clin Cancer Res* 17(20):6398–6405.
2. Kreitman RJ, et al. (2012) Phase I trial of anti-CD22 recombinant immunotoxin moxetumomab pasudotox (CAT-8015 or HA22) in patients with hairy cell leukemia. *J Clin Oncol* 30(15):1822–1828.
3. Reichert JM (2013) Antibodies to watch in 2013: Mid-year update. *MAbs* 5(4):513–517.
4. Chirino AJ, Ary ML, Marshall SA (2004) Minimizing the immunogenicity of protein therapeutics. *Drug Discov Today* 9(2):82–90.
5. De Groot AS, Scott DW (2007) Immunogenicity of protein therapeutics. *Trends Immunol* 28(11):482–490.
6. Hassan R, et al. (2007) Phase I study of SS1P, a recombinant anti-mesothelin immunotoxin given as a bolus I.V. infusion to patients with mesothelin-expressing mesothelioma, ovarian, and pancreatic cancers. *Clin Cancer Res* 13(17):5144–5149.
7. Kreitman RJ, Hassan R, Fitzgerald DJ, Pastan I (2009) Phase I trial of continuous infusion anti-mesothelin recombinant immunotoxin SS1P. *Clin Cancer Res* 15(16):5274–5279.
8. Kindt TJ, Osborne BA, Goldsby RA, eds (2000) *Kuby Immunology* (W. H. Freeman, New York), 6th Ed.
9. Parker DC (1993) T cell-dependent B cell activation. *Annu Rev Immunol* 11:331–360.
10. Yeung VP, et al. (2004) Elimination of an immunodominant CD4+ T cell epitope in human IFN-beta does not result in an in vivo response directed at the subdominant epitope. *J Immunol* 172(11):6658–6665.
11. Tangri S, et al. (2005) Rationally engineered therapeutic proteins with reduced immunogenicity. *J Immunol* 174(6):3187–3196.
12. Mazor R, et al. (2012) Identification and elimination of an immunodominant T-cell epitope in recombinant immunotoxins based on Pseudomonas exotoxin A. *Proc Natl Acad Sci USA* 109(51):E3597–E3603.
13. Chowdhury PS, Pastan I (1999) Improving antibody affinity by mimicking somatic hypermutation in vitro. *Nat Biotechnol* 17(6):568–572.
14. Weldon JE, et al. (2009) A protease-resistant immunotoxin against CD22 with greatly increased activity against CLL and diminished animal toxicity. *Blood* 113(16):3792–3800.
15. Wang P, et al. (2008) A systematic assessment of MHC class II peptide binding predictions and evaluation of a consensus approach. *PLOS Comput Biol* 4(4):e1000048.
16. Wedekind JE, et al. (2001) Refined crystallographic structure of Pseudomonas aeruginosa exotoxin A and its implications for the molecular mechanism of toxicity. *J Mol Biol* 314(4):823–837.
17. King C, et al. (2014) Removing T-cell epitopes with computational protein design. *Proc Natl Acad Sci USA* 111(23):8577–8582.
18. Lee B, Richards FM (1971) The interpretation of protein structures: Estimation of static accessibility. *J Mol Biol* 55(3):379–400.
19. Roscoe DM, et al. (1994) Primate antibody response to immunotoxin: Serological and computer-aided analysis of epitopes on a truncated form of Pseudomonas exotoxin. *Infect Immun* 62(11):5055–5065.
20. Weldon JE, et al. (2013) A recombinant immunotoxin against the tumor-associated antigen mesothelin reengineered for high activity, low off-target toxicity, and reduced antigenicity. *Mol Cancer Ther* 12(1):48–57.
21. Oseroff C, et al. (2010) Molecular determinants of T cell epitope recognition to the common Timothy grass allergen. *J Immunol* 185(2):943–955.
22. De Rosa SC, et al. (2004) Vaccination in humans generates broad T cell cytokine responses. *J Immunol* 173(9):5372–5380.
23. Kwok WW, et al. (2012) Frequency of epitope-specific naive CD4(+) T cells correlates with immunodominance in the human memory repertoire. *J Immunol* 188(6):2537–2544.
24. Harding FA (2008). US Patent 0153976.
25. Allured VS, Collier RJ, Carroll SF, McKay DB (1986) Structure of exotoxin A of Pseudomonas aeruginosa at 3.0-Angstrom resolution. *Proc Natl Acad Sci USA* 83(5):1320–1324.
26. Liu Z, Williams KP, Chang YH, Smith JA (1993) Immunodominance: A single amino acid substitution within an antigenic site alters intramolecular selection of T cell determinants. *J Immunol* 151(4):1852–1858.
27. Liu W, et al. (2012) Recombinant immunotoxin engineered for low immunogenicity and antigenicity by identifying and silencing human B-cell epitopes. *Proc Natl Acad Sci USA* 109(29):11782–11787.
28. Wang P, et al. (2010) Peptide binding predictions for HLA DR, DP and DQ molecules. *BMC Bioinformatics* 11:568.
29. Pastan I, Beers R, Bera TK (2004) Recombinant immunotoxins in the treatment of cancer. *Methods Mol Biol* 248:503–518.
30. Onda M, et al. (2011) Recombinant immunotoxin against B-cell malignancies with no immunogenicity in mice by removal of B-cell epitopes. *Proc Natl Acad Sci USA* 108(14):5742–5747.